



Experimental Study based Graphene Oxide Nanoplatelets Nanofluid Used in Domestic Application on the Performance of DASCs with Indirect Circulation Systems

S. khosrojerdi¹, A.M. Lavasani^{2*}, S. Delfani³, M. Vakili⁴

¹ Young Researchers' Club, Central Tehran Branch, Islamic Azad University, Tehran, Iran

² Department of Mechanics Engineering, Faculty of Technology and Engineering, Central Tehran Branch, Islamic Azad University, Tehran, Iran

³ Electrical and Mechanical Installations Department, Building and Construction Research Institute, Road, Housing and Urban Development Research Center, Tehran, Iran

⁴ School of Mechanical Engineering, Iran University of Science and Technology, Tehran, Iran

ABSTRACT: Since the solar energy is from the most well-known and important sources of clean energies, the solutions to absorb solar energy play significant role in the effectiveness of thermal collector system. The present study aims to investigate the experimental analysis of solar volume collector's performance for usage in domestic solar water heater and using graphene oxide nanoplatelets nanofluid based deionized water. The city of Tehran was the place for conducting experiments. The collector temperature ranges from 35 to 50 degrees Celsius under a clear sky. The uncertainty of experimental results was about 4.7 percent. The weight percentage of graphene oxide/deionized water has been chosen with the percentages of 0.005, 0.015 and 0.045, respectively. The used collector has been tested according to the standard of EN 12975-2 in different temperatures of inlet fluid and in flow rates of 0.0075, 0.015 and 0.225 kg/s. The results of this experiment determine that with the increase of nanofluid's weight percentage, the collector efficiency is increased and collector efficiency in its highest level in the flow rate of 0.015 kg/s and in the weight percentages of 0.005, 0.015 and 0.045 are 63.28, 72.59 and 75.07 respectively, which this amount for the base fluid is 58.25.

Review History:

Received: 7 April 2018

Revised: 23 September 2018

Accepted: 23 December 2018

Available Online: 1 February 2019

Keywords:

Direct absorption solar collector
Nanofluids
Graphene oxide nanoplatelets
Efficiency

1- Introduction

Searching for energy sources with lower environmental impact is in high demand in the hope of reducing carbon dioxide emission [1,2]. Using renewable resources is an important tool to achieve energy security, reducing greenhouse gas emissions and energy cost [3]. In this regard, the production of clean energies is of paramount importance. Solar energy as an infinite, free, clean and sustainable source of energy can be the best alternative to fossil fuels as permanent and clean energy [4,5]. Currently, a wide range of scientific research throughout the world is related to the issues on renewable energy sources such as solar collectors [6].

Study on the types of solar energy technologies proves that the conversion and using photo-thermal is of particular importance, because along with the use in heating systems [7], in electricity production [8] and chemical technology [9] has been used.

Collectors and absorbents are important components in solar thermal systems for converting photo-thermal. Volume absorbent or Direct Absorption Solar Collector (DASC) has high efficiency [10]. Suspended solid particles in DASCs will lead to an increment sun energy absorption [11]. The idea of suspending solid particle in a base fluid was introduced about a century ago which the mixture of nano particle and a base fluid is called "nanofluid" [12]. Several studies investigated effect of using nanofluid for heat transfer increment [13-17]. Effect of using graphite nanofluid in direct absorption

collector was first experimentally studied by Otanicar et al. [18]. Their results showed that using nanofluid would increase the efficiency of solar volume collector by 5% or more. Taylor et al. [19-25] showed that nanofluids have the ability of absorbing up to 95% of solar energy.

Mu et al. [26] through using the nanofluids of titanium oxide, zirconium oxide and silicon carbide based on water in volume collectors showed that the use of zirconium carbide nanoparticles in water would have significant impact to increase solar energy in comparison to other nanofluids. Optical properties of copper oxide nanofluid in low temperature experimentally investigated by Karami et al. [27]. They reported that the use of these nanoparticles in direct absorption systems would lead to system's improvement and the efficiency increase. Photothermal properties of graphene nanoplatelets nanofluids in Deionized (DI) water at low temperature DASCs experimentally studied by Vakili et al. [28]. Their results determined that 0.005 weight percentage of this nanofluid could absorb solar energy in the wavelength of 286 nm perfectly. Shendeh and Sundara [29] Showed that by using nano particles made of multi-wall carbon nanotube and graphene oxide thermal conductivity will increase up to 17.7%.

Said et al. [30] by experimental measured optical properties of nanofluid through metal oxide particles. They found that titanium oxide has superior properties compared to aluminum oxide. Karami et al. [31] suggested that using carbon nanotubes in DASCs with volume fraction of 150 Pmm would cause 32% increase heat transfer.

Corresponding author, E-mail: arashlavasani@iauctb.ac.ir

Lenert et al. [32] through using one-dimensional transient heat transfer model numerically solved a volume receiver in working high-temperature with absorption environment containing nanofluid. Their results determined that the nanofluid containing carbon nanoparticle covered with cobalt, would have the ability of absorbing 98% sun radiation.

Filho et al. [33] studied the importance of using silver nanoparticles in the enhancement of system performance and showed that nanofluid with volume fraction of 6.5 ppm would increase the performance of absorbent system by 144%.

Valiki et al. [34] experimentally investigated the use of graphene nanoplatelets nanofluid in volumetric solar collectors. They concluded that this nanofluid showed 93.24% of collector's efficiency in the best instance and this efficiency was 69.96% for the base fluid.

Delfani et al. [35] studied the application of Multi-Walled Carbon NanoTube (MWCNT) nanofluid in DASCs both experimentally and numerically. They reported that nanofluid would increase collector's efficiency from 10 to 29 % in comparison to base fluid. By using experimental and numerical method Gorji and Ranjbar [36] showed magnet and silver nanofluid would increase optical properties. Shende and Ramaprabhu [37] used of Nitrogen doped hybrid carbon based composite dispersed nanofluids in low temperature DASC for improving performance of solar collectors' efficiency. The optical properties of different nanofluids based ionic fluid was studied for finding a way to improve performance of medium to high working temperature DASCs [38]. Alumina nanofluid was used for improving efficiency of collectors at low working temperature [39,40].

By using numerical and experimental method the importance of using graphene nanofluid based ionic fluid in DASC at high working temperature [41]. They found the collector efficiency of 0.7 can be reached by using nanofluid with weight percentage of 0.0005 and at working temperature of 600 K.

Ladjevardi et al. [42] studied the application of graphite nanofluid in DASC which their studies indicate that using graphite nanofluid and volume fraction about 0.000025% could lead to absorption of more than 50% solar radiation energy.

Carbon nanostructures have higher thermal conductivity in comparison to other nanoparticles. The reason is the intrinsic thermal conductivity and lower density of particles or metal oxide as well as covalent bond and dispersion of more photons [43].

Considering the importance of working fluid and suspended particles in a volume or direct absorption collectors, the optimization of solar collectors by direct absorption mechanism occurs when an appropriate working fluid be used.

In the study of nanofluids for the applications of solar collectors, Nagarajan et al. [44] mentioned that the application of nanofluids to achieve highest probable thermal properties, in the lowest possible concentration with homogenous dispersion and stable suspension from nanoparticles in host liquid.

Hence, the importance of using graphene oxide nanoplatelets as working nanofluid in water without any surfactant for DASCs is studied in this work. The non-use of any 'surfactant' is one of the benefits of graphene nanofluid.

2- Experimental Method

2- 1- Materials

In this study, multi-layer graphene oxide nanoplatelets produced by US Research Nanomaterials, Inc., USA as working particle has been used which its characteristics have been shown in Table 1.

Table 1. Nanoparticles characteristics

Property	Characteristics
Type	Graphene Oxide
Appearance	Brown yellow or Black powder
Purity	99%
Layers	6-10 Layers
Diameter	10-50 nm
SSA	100-300 (m ² /gr)
Thickness	3.4-7 nm
Density	1 gr/cm ³
Volume Resistivity	4×10 ⁻⁴ ohm.cm

Considering the nature of nanofluid including a mix of nanoparticles and base fluid, heat transfer properties is the function of the properties of its components. Thus, real understanding of nanoparticles properties for using nanofluid in energy conversion systems is necessary [45]. They used Scanning Electron Microscope (SEM) and X-Ray diffraction methods for the structure analysis of nanoparticles. The scanning electronic microscope of AIS2100 (SEM), SERON TECHNOLOGIES INC, Gyeonggi-do, Korea has been used for finding the morphology of graphene oxide nanoplatelets' structure. SEM images have shown in Fig. 1.

To study the chemical compounds and crystal structure of nanoparticles, the device EQUINOX 3000, Inel INC, Artenay, France in measuring range of 5-120 degree has been used. The results are showed according to Fig. 2.

2- 2- Preparation method of nanofluid

Since the dispersion rate of nanoparticles in the base fluid for application in nanoparticles is of paramount importance, process of dispersing nanoparticles in fluid is consider as an important factor for finding nanofluid characteristics. For the nanofluid preparation of the current study a two-step process is used. In this method, nanoparticles by weight percentages of 0.005 (GO1), 0.015 (GO2) and 0.045 (GO3) in the based fluid which is deionized water are dispersed.

This process needs long mixing and use of ultrasonic systems ensuring uniform dispersion. For this reason, to disperse the nanoparticles, an ultrasonic system having the power of 770 watts and frequency of 20 kHz (Fig. 3) has been applied. The working time of Ultrasonic device for the production of samples is 45 minutes with power of 50%. In Figure. 4 shows prepared samples of nanofluid.

2- 3- Thermal conductivity of nanofluid

Thermal conductivity is an important parameter in many industrial and consumable systems. Basically, the poor thermal conductivity inherent in the normal fluids limits applications and effectiveness of heat transfer [46].

Suspended nanoparticles in fluid increases rate of heat transfer due to increment of thermal conductivity and surface area of the particles. Effect of increasing nanofluid

weight percentage on thermal conductivity and heat transfer increment is investigated this part. Graphene oxide nanofluid was measured at temperatures 25 to 50 °C in different weight

percentages which the results of experimental measurement are shown in Fig. 5.

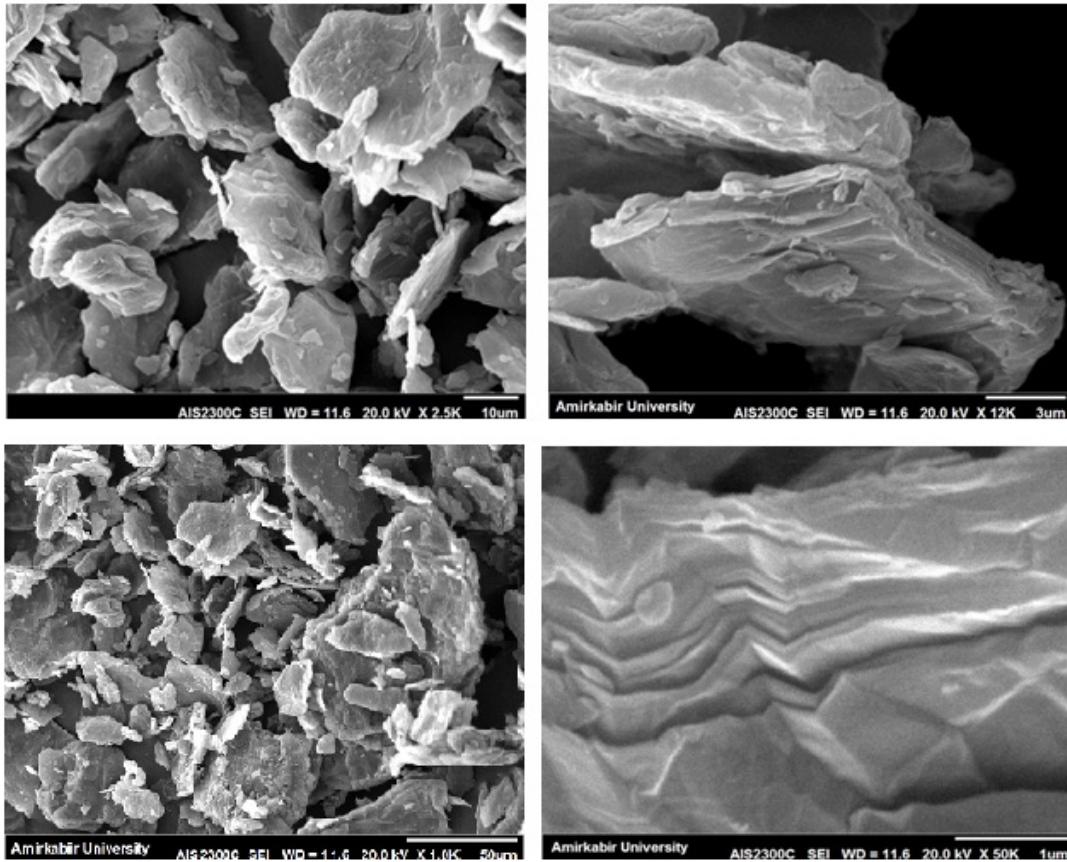


Fig. 1. SEM images of graphene oxide nanoplatelets

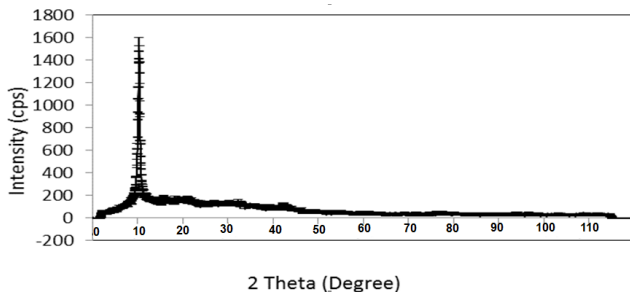


Fig. 2. X-Ray Diffraction of graphene oxide nanoplatelets



Fig. 3. Ultrasonic Q700 Sonicator equipment

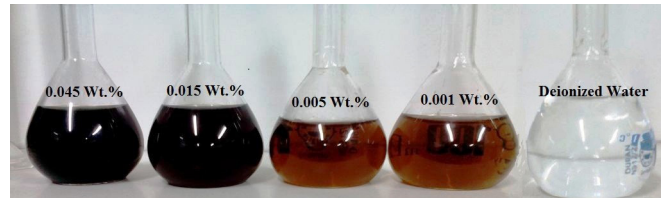


Fig. 4. The image of nanofluid samples with different weight percentages

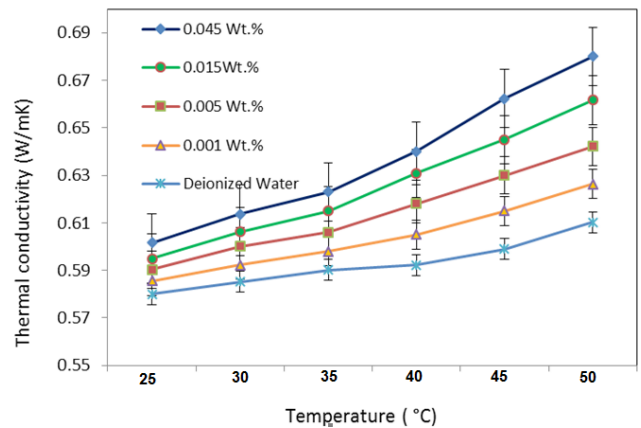


Fig. 5. Thermal conductivity of sample nanofluids and deionized water at different temperatures

The dependency of thermal conductivity with nanofluid temperature can be observed in Figure 5 whereas by increasing the temperature, thermal conductivity of nanofluid increases. One of the reasons for this dependency to the temperature is that as the temperature increases the movement and oscillation of nanoparticles with also increase. So that with increasing temperature, Brownian motion of nanoparticles increases and the viscosity of base fluid decreases. Nanofluid morphology in the current study is sheet like which can behave as a bridge to heat transfer. Therefore, Heat transfer will increase with the increase of the weight percentage of nanofluid. Fig. 6 represents the percentage of heat transfer coefficient increment at temperature of 25°C and 50°C for various weight percentage.

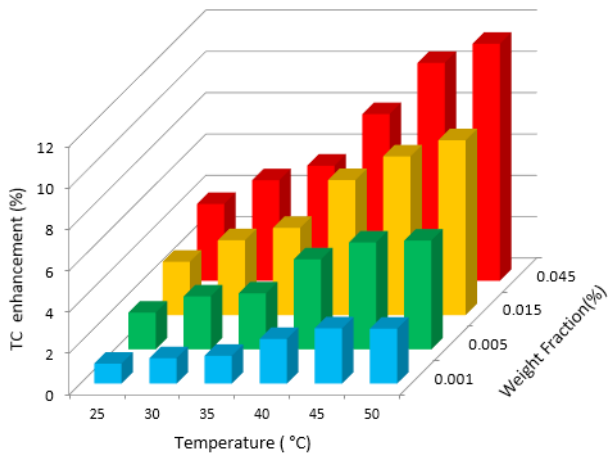


Fig. 6. Increase percentage of nanofluid's thermal conductivity with different nanoparticle weight percentages in temperatures 25°C to 50°C

As it is clear from Fig. 6, thermal conductivity measured with weight percentages 0.001, 0.005, 0.015 and 0.045 in temperatures 25-50 °C in each 5 °C that results showed with the increase of weight percentage, the increase of thermal conductivity in high temperature is more prominent. The cause for this is increasing thermal conductivity of base fluid and also the thermal conductivity of nanoparticles is also increased with temperature increase.

2- 4- Stability of nanofluid

In this study, graphene oxide having honeycomb structure which shows high electrical conductive property due to the free electrons as well as high suspension and very suitable stability of this nanofluid has been used to test in solar collector.

The study of electrophoretic behavior, which can be evaluated by measuring Zeta potential, is considerably crucial in understanding the dispersion behavior of nanoparticles inside liquid environment.

Fluids contain ions or atoms, which can have positive or negative charges.

In fluid environment with dispersing the particles, the ions which are charged move towards the particles with opposite charge and are absorbed to them which this lead to agglomeration phenomenon in nanofluid. The zeta potential is a key indicator of the stability of colloidal dispersions. The magnitude of the zeta potential indicates the degree of electrostatic repulsion between adjacent, similarly charged

particles in a dispersion. The stability of a colloidal system is determined by the sum of Van Der Waals attraction forces and electrical two-layer disposal forces. Generally, Zeta potential is introduced as the amount of stability border, which is from -25 Mv to +25 Mv [47]. So that, the nanofluid with Zeta potential over +30 and below -30 is suitably stable [12].

In this study Zeta potential was measured using a ZEN3600 Zetasizer from Malvern Company, UK. This equipment can measure the size range for zeta potential of 5 nm to 10 microns and Size range of 0.6 nm to 6 microns for other particles dispersed in the solution.

In this study, it can be concluded from the conducted experiment that the Zeta potential of the nanofluid which is prepared from graphene oxide is -39.2, indicating appropriate stability for nanofluid to utilize in heating systems. The results of measurement are based on Fig. 7.

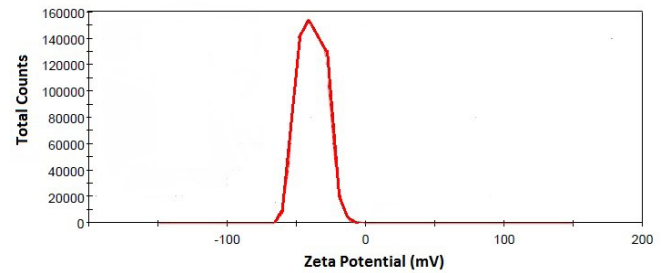


Fig. 7. Results of measuring zeta potential for nanofluid with weight percentage of 0.015

Anin Vincely et al. [43] utilized graphene oxide nanofluid for flat plate solar collectors, and reported that this nanofluid had been observed for 60 days without no sediment.

Said, Z., et al. [48] with using titanium dioxide nanofluid and Polyethylene Glycol dispersant investigated performance enhancement of a Flat Plate Solar collector and reported that TiO₂-H₂O nanofluid sustained stable for a period of more than one month.

The prepared 200 cc sample of it by authors had kept its stability after 440 days, which is shown in Fig. 8.



Fig. 8. Photograph of graphene oxide nanoplatelets nanofluid GO3, after 440 days

Therefore, this nanofluid, which have the increasing heat transfer, was chosen to test since it was a suitable opinion concerning stability for being applicable in collector. By examining other aspects it can be stated definitive opinion about this. By preparing nanofluid containing graphene oxide

nanoplatelet based deionized water with three different weight percentages of 0.005, 0.015 and 0.045, the performance and experimental analysis of DASC investigated with the aim of using in domestic solar water heater.

3- Characteristics of Experiment's Equipment

In order to experimentally study the performance of DASC, one sample of it with the aim of using in domestic solar water heater placed at Tehran city (35.6961° N, 51.4231° E) has been used. The installation angle of collector to receive most solar radiation has been designed and built equal to latitude of Tehran (35°).

According to the picture which is shown in Fig. 9, DASC has dimensions of 60 by 60 cm and depth of 10 mm and a body made of aluminum and collector's body has been fully insulated using polyurethane insulation with a thickness of 10 mm to restrict the heat loss to the environment which is outside of back and side walls.



(a)



(b)

Fig. 9. Photographs of equipment of experiment- a) pretest b) testing with graphene oxide nanoplatelets nanofluid

To measure solar radiation hemisphere, the pyranometer of CMP-Kipp & Zonen with uncertainty $5/3\% \pm$ has been used. Since the measurement is done in outside environment, the measurement sensor of ambient air temperature is protected from direct and reflected solar radiation by reflector canopy (laminated with aluminum foil).

The sensor for measuring temperature has not more than 200 mm distance from collector (number 3 & 10 in Fig. 10) input and insulation around upstream and downstream sensor pipe has been done.

An electrical pump and a flow control valve are used to maintain the flow rate through the collector stable to within 1%. The fluid flow rate was measured with a turbine flow meter (Lico-vision 1000 series) with an accuracy of $\pm 1\%$. This flow meter is used for flow rates up to 2.5 lit/min.

4- Experimental Investigation

Among the types of experiment's standards and methods in this research, the experiment has been done according to EN 12975-2 standard [49] which the schema-shaped of experiment device with test equipment layout is shown in Fig. 10.

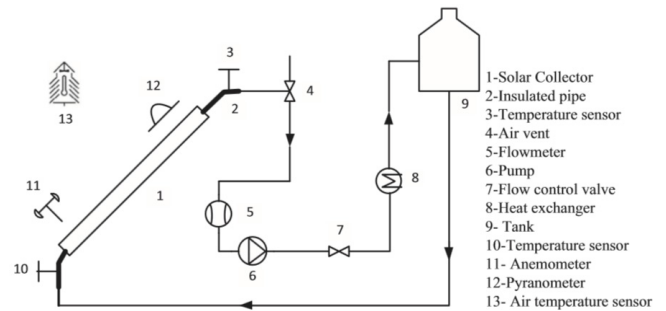


Fig. 10. Schematic of experimental equipment

Collector experiment ranging in working temperature ranging is from 35 to 50 °C under a clear sky and in accordance with the conditions that must be kept constant during the experiment as shown in Table 2.

Table 2. Allowed deviation of determined parameters during a measurement period (EN 12975-2 Standard [49])

Parameter	Permitted deviation of measured
Global test solar irradiance (W/m)	± 50
Surrounding air temperature (°C)	± 1.5
Fluid mass flow rate (%)	± 1
Fluid temperature at the collector inlet & outlet (°C)	± 0.1
Wind speed (m/s)	2-4

The experiment method is firstly after making sure of suitable conditions, collector is protected by use of a reflective coating (aluminum foil) and the canopy's umbrella against the sun until the steady conditions and we achieved and input and output temperature be equal, then the coating quickly is removed from collector and measurements are continued to achieve secondary steady-state conditions.

4- 1- Time of experiment

The experiment's time to achieve steady data points should include pre-data interval and at least four times the collector's time (or at least 15 minutes if the time constant is not known) and data interval or experiment's time be at least four times the collector's time (it should not be less than 10 minutes when the time constant is unknown).

Collector's time constant as the time is elapsed till the temperature difference of ambient air and effluent from collector is achieved to 63.2 which are equal to the subtraction of ambient air's temperature difference and initial output temperature and ambient air's time difference and secondary output temperature. Collector's time constant is obtained using Eq. (1).

$$\tau = 0.632 \times \left((T_{out} - T_{amb})_2 - (T_{out} - T_{amb})_1 \right) \quad (1)$$

Regarding the Fig. 11 and results of measurement, time constant is 3.53 which according to the standard of pre-experiment (pre-test) and experiment are 4 times to it which for each of pre-experiment and experiment will be about 14 to 15 minutes.

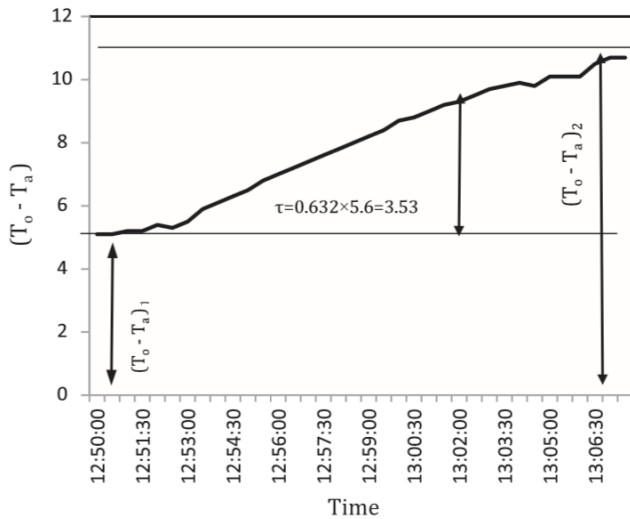


Fig. 11. Time constant graph of collector

4- 2- Computing collector's efficiency

To compute collector's efficiency, data points (given points) for at least 4 input temperatures chosen uniformly in the range of collector's working temperature have been used. In order to reach the highest efficiency, the first input temperature has been chosen as much as the ambient temperature. To draw the collector's curve fitting of efficiency, 4 independent data have been used for each input temperature which in total they are 16 data points in 4 input temperatures.

The real extracted power is calculated by Eq. (2):

$$\dot{Q} = \dot{m} C_p (T_{out} - T_{in}) \frac{-b \pm \sqrt{b^2 - 4ac}}{2a} \quad (2)$$

The specific heat of nanofluid can be calculated through theory relations. Regarding the conducted studies by Honly (STANDARD, 2006) about the models and relation utilized

to predict specific heat, in this research Eq. (3) has been used to calculate:

$$C_{p,nf} = \frac{\phi(\rho C_p)_n + (1-\phi)(\rho C_p)_f}{\phi\rho_n + (1-\phi)\rho_f} \quad (3)$$

Solar energy received by collector is $A_G G_T$ in which A_G is collector's surface. Considering the collector's suitable power can be written as following:

$$\eta_G = \frac{\dot{m} C_p (T_{out} - T_{in})}{A_G G_T} \quad (4)$$

To investigate collector's performance, drawing efficiency graph is done according to a function of decreased temperature:

$$T_m = T_{in} + \frac{T_{out} - T_{in}}{2} \quad (5)$$

$$T_m^* = \frac{T_m - T_a}{G_T} \quad (6)$$

According to the standard of EN-12975-2[49], moment thermal efficiency in terms of reduced temperature difference is expressed as following:

$$\eta = \eta_0 - a_1 T_m^* - a_2 G_T (T_m^*)^2 \quad (7)$$

The variables of a_1 and a_2 by use of the statistical curve fitting of experimental data with the method of least squares are obtained as linear or quadratic. The intersection of efficiency (performance) graph with vertical axis indicates η_0 or the same most efficiency. On the other hand, the efficiency graph slope will be equal to a_1 , meaning the heat loss coefficient from collector [49] (STANDARD, 2006).

Since the efficiency of the collector is dependent to the mass flow rate (flow) rate, output and input temperatures as well as sun's radiation, Eq. (8) has been used to study the combined uncertainty of experimental results which this amount with respect to conducted calculations is 4.7%:

$$U_\eta = \sqrt{U_m^2 + U_{GT}^2 + U_{\Delta T}^2} \quad (8)$$

where U_m , U_{GT} and $U_{\Delta T}$ are the uncertainties of \dot{m} , G_T and ΔT , respectively, all of which are expressed in percent (i.e., relative error with respect to the average values) and each consists of fixed error which is caused by error of the measuring equipment's and random error which is caused by data scattering due to random fluctuation of the process

$$U_i = \sqrt{U_{i,f}^2 + U_{i,r}^2} \quad (9)$$

$U_{i,f}$ represents the fixed error of the i th component; $U_{i,r}$, represents the random error of the i th component.

Each parameter has its uncertainty, including fixed and variable errors. The mass flow rate (flow) rate measurement error, which is related to measuring equipment and it is

known as fixed error, equals to $\pm 1.0\%$ random error led by the way of measurement and experiment equals to less than 1.9 percent. Fixed error to measure input and output temperatures equals $\pm 0.1\text{ }^\circ\text{C}$ and random error of $\Delta T < 1\text{ }^\circ\text{C}$. Ultimately, the radiation that is emitted from the sun with fixed error from -3.5% to $+3.5\%$, and random error which is less than 2% have been used in this experiment.

In Table 3, a summary of these results has been shown.

Table 3. Uncertainty of parameter's measurement results

Parameter	fixed error	random error	(U)
m	$\pm 1\%$	$1.9 < \%$	2.17%
ΔT	$\pm 0.1\text{ }^\circ\text{C}$	$< 1\text{ }^\circ\text{C}$	1.01 $^\circ\text{C}$
G_T	$\pm 3.5\%$	$2\% <$	4.07%

5- Results

5- 1- Base fluid performance

Since in this experimental work, deionized water has been used as base fluid, this section has investigated the performance and results of deionized water without the presence of working particles in collector.

The results of experiment in different flow rates (base fluid) are shown in Fig. 12. According to the results of collector's efficiency with deionized water it can be concluded that efficiency in flow rate of 0.0075 kg/s and in flow rate of 0.015 would be the lowest and highest amount. As it is clear from the results, flow rate's increase necessarily wouldn't increase collector's efficiency, because by increasing more than optimal amount, the fluid would have less chance for being exposed by sun's radiation. So, the conclusion is that the optimal amount of flow rate among selected amounts is 0.015 kg/s.

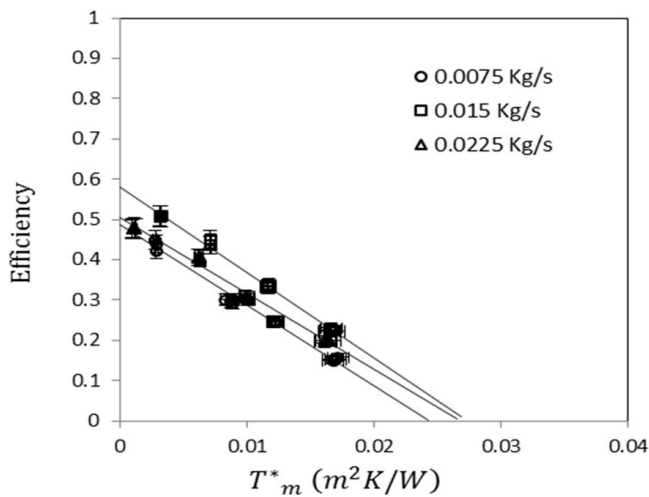


Fig. 12. Collector's efficiency with base fluid in different flow rates

5- 2- Examining the effect of nanofluid's performance in comparison to base fluid

The impact of utilizing nanofluid (weight percentage of 0.045) as collector's working fluid in comparison with base fluid for three various flow rates has been examined in Figs. 8 to 10.

Results suggest that in all input flow rates the efficiency compared to base fluid would be increased through using

graphene oxide nanoplatelets nanofluids.

Highest efficiencies by use of base fluid and nanofluid in flow rate 0.0075 kg/s are 0.48 and 0.62, and; in flow rate 0.015 kg/s are 0.58 and 0.75 and; in flow rate 0.0225kg/s are 0.50 and 0.73, respectively.

Nanofluid in its highest weight percentage (0.045 Wt.%) and in flow rate 0.0075kg/s has increased 29.16, in flow rate 0.015kg/s has increased 29.31 and in flow rate 0.0225kg/s has increased 46.01 of collector's efficiency. This approved that nanofluid has more ability to absorb solar radiation than base fluid.

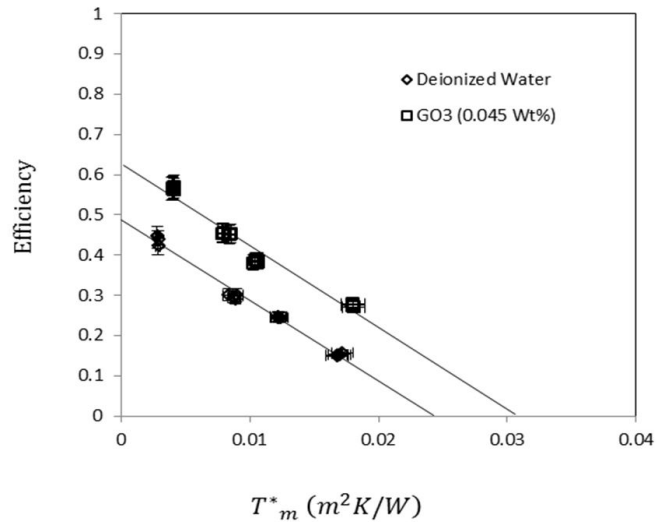


Fig. 13. Effect of GO3 nanofluid on direct absorption solar collector's efficiency (at 0.0075kg/s flow rate)

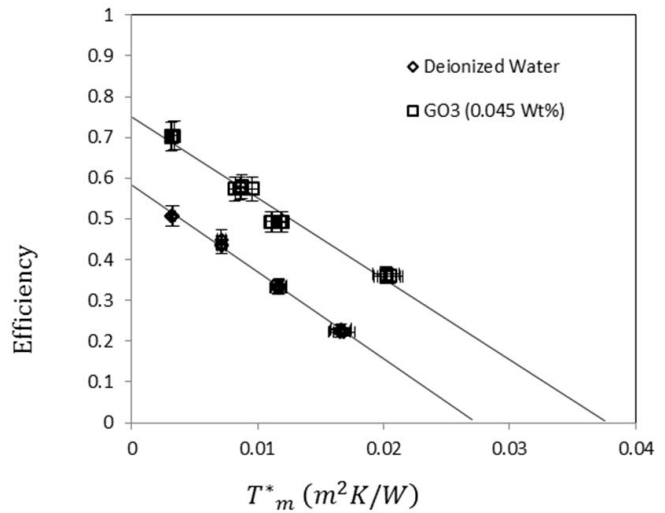


Fig. 14. Effect of GO3 nanofluid on direct absorption solar collector's efficiency (at 0.015kg/s flow rate)

5- 3- Examining the impact of nanofluid's weight percentage

In Fig. 16 the impact of nanofluid's weight percentage on direct absorption collector at 0.015 kilogram per second flow rate has been shown. According to the results of collector's testing, the more nanofluid is tick, sun's energy absorption is greater and consequently, efficiency will be increased.

Collector's efficiency at its highest amount, through using GO1, GO2 and GO3 nanofluids at 0.015kg/s flow rate was

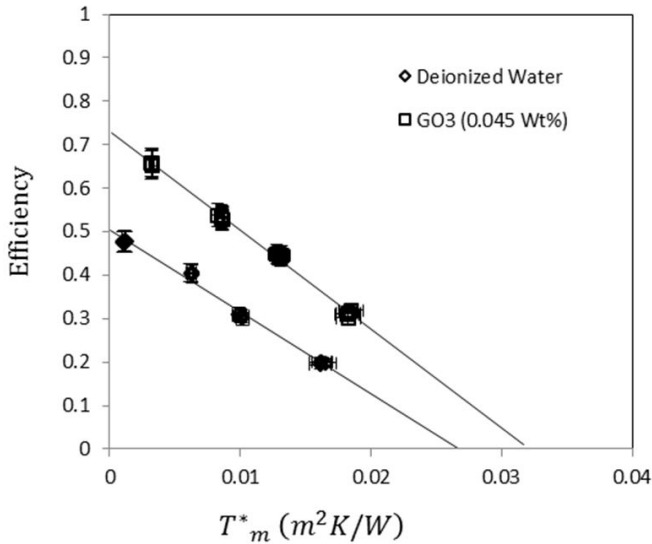


Fig. 15. Effect of GO3 nanofluid on direct absorption solar collector's efficiency (at 0.0225kg/s flow rate)

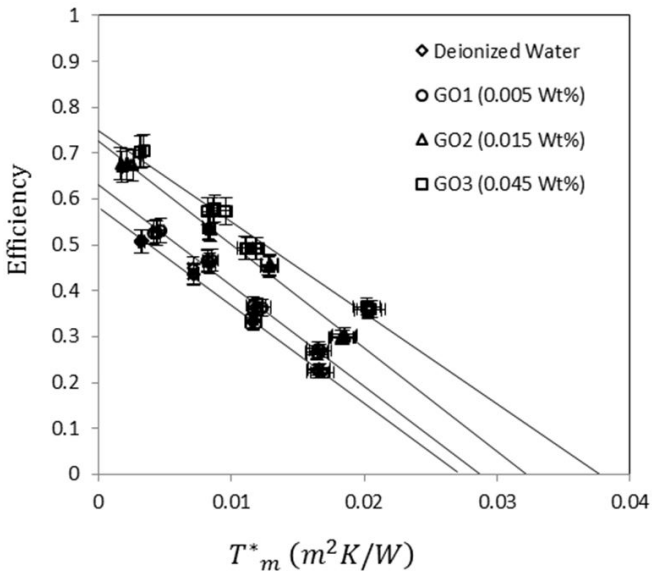


Fig. 16. Impact of nanofluid's weight percentage on collector's efficiency (at 0.015kg/s flow rate)

63.28, 72.59 and 75.07, respectively. This amount for base fluid is 58.25.

5- 4- Investigating the effect of input flow rate

Fig. 17 shows efficiency's changes based on the reduced temperature difference for different flow rate of 0.0075 kg/s, 0.015kg/s and 0.0225. The results suggest that the effect of flow rate on collector's efficiency level using nanofluid is in accordance with the results of base fluid, meaning that collector's efficiency in flow rate of 0.0075 has the lowest amount and in flow rate of 0.015 has highest amount.

Highest collector's efficiency in all conditions related to GO3 nanofluid is in the flow rate of 0.015kg/s which this amount is equal to 75%. Heat loss coefficient of α_1 , in the flow rate of 0.015kg/s, 0.0225kg/s and 0.0075kg/s have the difference about 2 percentage to one another which this amount is inconsiderable. The highest heat loss is linked to GO2 nanofluid with flow rate of 0.0225 kilogram per second.

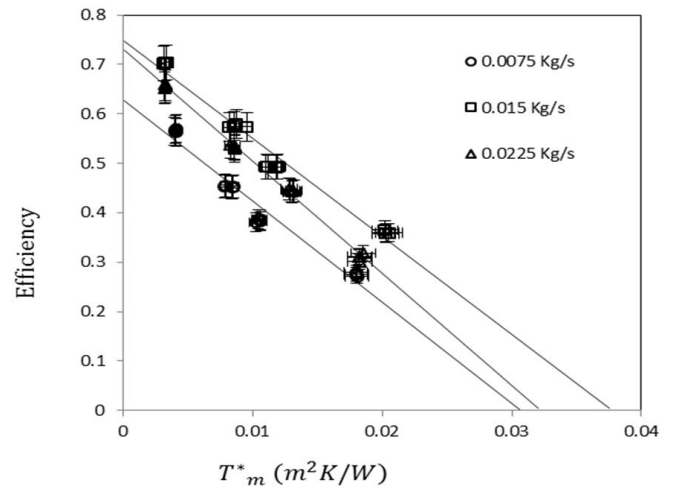


Fig. 17. Effect of Working Fluid on the Direct Absorption's Efficiency (weight percentage of 0.045)

6- Conclusion

In this study, the performance of DASC with the aim of using it in domestic solar water heater and by use of graphene oxide nanosheets/deionized water with different weight percentages as working fluid has been investigated which the results of experimental analysis are as following:

- Collector efficiency by use of nanofluid has been increased in all flow rates.
- Collector efficiency by use of nanofluid has been increased by increasing nanofluid's weight percentages.
- Investigation shows that flow rate increase has not lead to collector efficiency increase. Since, by the increase of flow rate, the working fluid has less chance for receiving sun radiation.
- The effect of collector's efficiency by use of nanofluid is according to the results of base fluid, meaning that collector's efficiency in flow rate 0.0075kg/s would have the lowest amount and in flow rate 0.015kg/s will have highest amount.
- The highest collector's efficiency in all conditions is related to nanofluid GO3 in flow rate of 0.015kg/s which is equal to 75% and the highest loss heat coefficient is related to nanofluid GO2 with flow rate of 0.0225kg/s.

References

- [1] G. Coccia, G. Di Nicola, L. Colla, L. Fedele, M.J.E.C. Scattolini, Management, Adoption of nanofluids in low-enthalpy parabolic trough solar collectors: numerical simulation of the yearly yield, 118 (2016) 306-319.
- [2] Z. Said, M. Sabiha, R. Saidur, A. Hepbasli, N. Rahim, S. Mekhilef, T.J.J.o.C.P. Ward, Performance enhancement of a flat plate solar collector using titanium dioxide nanofluid and polyethylene glycol dispersant, 92 (2015) 343-353.
- [3] V. Drosou, P. Kosmopoulos, A.J.R.E. Papadopoulos, Solar cooling system using concentrating collectors for office buildings: A case study for Greece, 97 (2016) 697-708.
- [4] M. Karamali, M.J.R.E. Khodabandeh, A distributed solar collector field temperature profile control and estimation using inlet oil temperature and radiation estimates based on Iterative Extended Kalman Filter, 101 (2017) 144-

- 155.
- [5] Z. Said, R. Saidur, N.J.J.o.C.P. Rahim, Energy and exergy analysis of a flat plate solar collector using different sizes of aluminium oxide based nanofluid, 133 (2016) 518-530.
- [6] M. Nemš, J.J.R.E. Kasperski, Experimental investigation of concentrated solar air-heater with internal multiple-fin array, 97 (2016) 722-730.
- [7] J.A. Duffie, W.A. Beckman, Solar engineering of thermal processes, John Wiley & Sons, 2013.
- [8] J. Ji, J.-P. Lu, T.-T. Chow, W. He, G.J.A.E. Pei, A sensitivity study of a hybrid photovoltaic/thermal water-heating system with natural circulation, 84(2) (2007) 222-237.
- [9] P.V.J.T.J.o.P.C.C. Kamat, Meeting the clean energy demand: nanostructure architectures for solar energy conversion, 111(7) (2007) 2834-2860.
- [10] T.P. Otanicar, J.S.J.E.s. Golden, technology, Comparative environmental and economic analysis of conventional and nanofluid solar hot water technologies, 43(15) (2009) 6082-6087.
- [11] W. Minkowycz, E.M. Sparrow, J.P. Abraham, Nanoparticle heat transfer and fluid flow, CRC press, 2016.
- [12] S.K. Das, S.U. Choi, W. Yu, T. Pradeep, Nanofluids: science and technology, John Wiley & Sons, 2007.
- [13] A. Beheshti, M. Shanbedi, S.Z.J.J.o.T.A. Heris, Calorimetry, Heat transfer and rheological properties of transformer oil-oxidized MWCNT nanofluid, 118(3) (2014) 1451-1460.
- [14] M. Mehrali, E. Sadeghinezhad, S.T. Latibari, S.N. Kazi, M. Mehrali, M.N.B.M. Zubir, H.S.C.J.N.r.l. Metselaar, Investigation of thermal conductivity and rheological properties of nanofluids containing graphene nanoplatelets, 9(1) (2014) 15.
- [15] R. Mohebbi, M.J.J.o.t.T.I.o.C.E. Rashidi, Numerical simulation of natural convection heat transfer of a nanofluid in an L-shaped enclosure with a heating obstacle, 72 (2017) 70-84.
- [16] R. Mohebbi, M. Rashidi, M. Izadi, N.A.C. Sidik, H.W.J.I.J.o.H. Xian, M. Transfer, Forced convection of nanofluids in an extended surfaces channel using lattice Boltzmann method, 117 (2018) 1291-1303.
- [17] M. Izadi, R. Mohebbi, D. Karimi, M.A.J.C.E. Sheremet, P.-P. Intensification, Numerical simulation of natural convection heat transfer inside a \perp shaped cavity filled by a MWCNT-Fe₃O₄/water hybrid nanofluids using LBM, 125 (2018) 56-66.
- [18] T.P. Otanicar, P.E. Phelan, R.S. Prasher, G. Rosengarten, R.A.J.J.o.r. Taylor, s. energy, Nanofluid-based direct absorption solar collector, 2(3) (2010) 033102.
- [19] R.A. Taylor, P.E. Phelan, T.P. Otanicar, R. Adrian, R.J.N.r.l. Prasher, Nanofluid optical property characterization: towards efficient direct absorption solar collectors, 6(1) (2011) 225.
- [20] R. Mohebbi, M. Nazari, M.J.J.o.A.M. Kayhani, T. Physics, Comparative study of forced convection of a power-law fluid in a channel with a built-in square cylinder, 57(1) (2016) 55-68.
- [21] R. Mohebbi, H.J.I.J.o.M.P.C. Heidari, Lattice Boltzmann simulation of fluid flow and heat transfer in a parallel-plate channel with transverse rectangular cavities, 28(03) (2017) 1750042.
- [22] R. Mohebbi, H. Lakzayi, N.A.C. Sidik, W.M.A.A.J.I.J.o.H. Japar, M. Transfer, Lattice Boltzmann method based study of the heat transfer augmentation associated with Cu/water nanofluid in a channel with surface mounted blocks, 117 (2018) 425-435.
- [23] R. Mohebbi, M. Izadi, A.J.J.P.o.F. Chamkha, Heat source location and natural convection in a C-shaped enclosure saturated by a nanofluid, 29(12) (2017) 122009.
- [24] Y. Ma, R. Mohebbi, M. Rashidi, Z.J.P.o.F. Yang, Study of nanofluid forced convection heat transfer in a bent channel by means of lattice Boltzmann method, 30(3) (2018) 032001.
- [25] Y. Ma, R. Mohebbi, M. Rashidi, Z.J.I.J.o.M.P.C. Yang, Numerical simulation of flow over a square cylinder with upstream and downstream circular bar using lattice Boltzmann method, 29(04) (2018) 1850030.
- [26] L. Mu, Q. Zhu, L. Si, Radiative properties of nanofluids and performance of a direct solar absorber using nanofluids, in: ASME 2009 Second International Conference on Micro/Nanoscale Heat and Mass Transfer, American Society of Mechanical Engineers, 2009, pp. 549-553.
- [27] M. Karami, M. Akhavan-Bahabadi, S. Delfani, M.J.R. Raisee, S.E. Reviews, Experimental investigation of CuO nanofluid-based Direct Absorption Solar Collector for residential applications, 52 (2015) 793-801.
- [28] M. Vakili, S. Hosseinalipour, S. Delfani, S.J.S.E.M. Khosrojerdi, S. Cells, Photothermal properties of graphene nanoplatelets nanofluid for low-temperature direct absorption solar collectors, 152 (2016) 187-191.
- [29] R. Shende, R.J.S.E.M. Sundara, S. Cells, Nitrogen doped hybrid carbon based composite dispersed nanofluids as working fluid for low-temperature direct absorption solar collectors, 140 (2015) 9-16.
- [30] Z. Said, R. Saidur, N.J.I.C.i.H. Rahim, M. Transfer, Optical properties of metal oxides based nanofluids, 59 (2014) 46-54.
- [31] M. Karami, M.A. Bahabadi, S. Delfani, A.J.S.E.M. Ghozatloo, S. Cells, A new application of carbon nanotubes nanofluid as working fluid of low-temperature direct absorption solar collector, 121 (2014) 114-118.
- [32] A. Lenert, Y.S.P. Zuniga, E.N. Wang, Nanofluid-based absorbers for high temperature direct solar collectors, in: 2010 14th International Heat Transfer Conference, American Society of Mechanical Engineers, 2010, pp. 499-508.
- [33] E.P. Bandarra Filho, O.S.H. Mendoza, C.L.L. Beicker, A. Menezes, D.J.E.C. Wen, Management, Experimental investigation of a silver nanoparticle-based direct absorption solar thermal system, 84 (2014) 261-267.
- [34] S. Delfani, M. Karami, M.J.R.E. Akhavan-Behabadi, Performance characteristics of a residential-type direct absorption solar collector using MWCNT nanofluid, 87 (2016) 754-764.

- [35] T.B. Gorji, A.J.S.E. Ranjbar, A numerical and experimental investigation on the performance of a low-flux direct absorption solar collector (DASC) using graphite, magnetite and silver nanofluids, 135 (2016) 493-505.
- [36] R.C. Shende, S.J.S.E.M. Ramaprabhu, S. Cells, Thermo-optical properties of partially unzipped multiwalled carbon nanotubes dispersed nanofluids for direct absorption solar thermal energy systems, 157 (2016) 117-125.
- [37] L. Zhang, J. Liu, G. He, Z. Ye, X. Fang, Z.J.S.E.M. Zhang, S. Cells, Radiative properties of ionic liquid-based nanofluids for medium-to-high-temperature direct absorption solar collectors, 130 (2014) 521-528.
- [38] H.K. Gupta, G.D. Agrawal, J.J.S.E. Mathur, An experimental investigation of a low temperature Al₂O₃-H₂O nanofluid based direct absorption solar collector, 118 (2015) 390-396.
- [39] H.K. Gupta, G.D. Agrawal, J.J.C.S.i.T.E. Mathur, Investigations for effect of Al₂O₃-H₂O nanofluid flow rate on the efficiency of direct absorption solar collector, 5 (2015) 70-78.
- [40] J. Liu, Z. Ye, L. Zhang, X. Fang, Z.J.S.E.M. Zhang, S. Cells, A combined numerical and experimental study on graphene/ionic liquid nanofluid based direct absorption solar collector, 136 (2015) 177-186.
- [41] S. Ladjevardi, A. Asnaghi, P. Izadkhist, A.J.S.E. Kashani, Applicability of graphite nanofluids in direct solar energy absorption, 94 (2013) 327-334.
- [42] D.A. Vincely, E.J.E.c. Natarajan, management, Experimental investigation of the solar FPC performance using graphene oxide nanofluid under forced circulation, 117 (2016) 1-11.
- [43] P. Nagarajan, J. Subramani, S. Suyambazhahan, R.J.E.P. Sathyamurthy, Nanofluids for solar collector applications: a review, 61 (2014) 2416-2434.
- [44] M. Tahani, M. Vakili, S.J.I.C.i.H. Khosrojerdi, M. Transfer, Experimental evaluation and ANN modeling of thermal conductivity of graphene oxide nanoplatelets/deionized water nanofluid, 76 (2016) 358-365.
- [45] S.S. Park, N.J.J.R.e. Kim, A study on the characteristics of carbon nanofluid for heat transfer enhancement of heat pipe, 65 (2014) 123-129.
- [46] W. Yu, H.J.J.o.n. Xie, A review on nanofluids: preparation, stability mechanisms, and applications, 2012 (2012) 1.
- [47] Z. Said, R. Saidur, M. Sabiha, A. Hepbasli, N.J.J.o.c.p. Rahim, Energy and exergy efficiency of a flat plate solar collector using pH treated Al₂O₃ nanofluid, 112 (2016) 3915-3926.
- [48] B.J.B.S.I. EN12975, 2. Thermal solar systems and components solar collectors-Part 2: test methods FS, (2001).

Please cite this article using:

S. khosrojerdi, A.M. Lavasani, S. Delfani, M. Vakili, Experimental Study based Graphene Oxide Nanoplatelets Nanofluid Used in Domestic Application on the Performance of Direct Absorption Solar Water Heaters with Indirect Circulation Systems, *AUT J. Mech. Eng.*, 3(1) (2019) 43-52.
DOI: 10.22060/ajme.2018.14289.5720

